

IMPERIAL COLLEGE OF SCIENCE AND TECHNOLOGY

Department of Aeronautics

Prince Consort Road, London, SW7 2BY England

Semi-Annual Status Report on

Research Grant No. NAGW-581

"Vortex Boundary-Layer Interactions"

Period 1 March 1985 - 31 August 1985

P. Bradshaw, Principal Investigator

NASA-CR-176192
19850027060

LIBRARY COPY

MAR 7 1986

LANGLEY RESEARCH CENTER
LIBRARY, NASA
HAMPTON, VIRGINIA



NF01770

Summary

The purpose of this work is to study the interaction of a turbulent boundary layer - on a flat plate - with a strong artificially generated longitudinal vortex which may or may not actually enter the boundary layer. The vortices are generated by a delta wing suspended ahead of the test plate, so that the configuration is approximately that of a close-coupled canard with zero main-wing sweep and an invisible body. At the time of writing the post doctoral research assistant has been in post for just over twelve months, all necessary configuration and parametric checks have been completed, and data acquisition and analysis on the first configuration chosen for detailed study - in which the vortex starts to merge with the boundary layer a short distance downstream of the leading edge of the test plate - are nearly complete.

Present position

Figure 1, repeated from previous progress reports for convenience, shows the test configuration. The non-rolled-up part of the delta wing wake passes underneath the test plate, so that the boundary layer on the test plate between the vortices is nominally undisturbed, except by very strong lateral divergence in the induced flow field of the vortices (surface cross-flow angles exceed 30°).

Hot-wire measurements are made with the on-line data logging and analysis system described in previous progress reports, currently based on an IBM PC clone: all three mean velocity components, all six independent Reynolds stresses, and all ten independent triple products are stored on floppy discs for on-line plotting. Figures 2 to 6 show sample results at one streamwise station at an external-stream speed of about 16 m/s. It seems to be conventional to think of vortices as rotating in the clockwise direction, and the presentation has been changed from that used in previous reports so that the left-hand vortex of the pair generated by the delta-wing is shown in the figures, and the "common" flow is on the right, downwards toward the test-plate. The axis of symmetry of the flow is close to $Z=0$ inches, and the left-hand side wall is at $Z \approx -16.75$ inches. Figures 2(a) and 2(b) show the same results, to different scales: figure 2(a) shows the cross flow velocities in the vortex core region, whereas figure 2(b) is plotted to show up the weaker cross flow further from the core. Figure 3, showing the axial-component mean velocity, is interestingly different from the total-pressure contours previously presented: the latter (which look very roughly like the turbulent kinetic energy contours in figure 5) actually give a more useful indication of the boundary of the turbulent region. The region of low total pressure in the vortex core is also a region of very low static pressure, and therefore of high axial mean velocity. This is an unavoidable consequence of the process of vortex generation, and although a classical trailing vortex with negligible longitudinal-velocity perturbations might have been academically preferable, the delta-wing vortex is presumably quite similar to a

typical strake-wing vortex. The "tongue" of low-velocity fluid that projects away from the surface at $z=-8$ " approximately in figure 3 also shows up as a region of low total pressure, lying between the primary vortex and the secondary vortex whose effects are just discernable in figure 2(b) near $z=-10$ ".

Figure 4 shows contours of the three components of shear stress, (strictly $(-1/\rho)$ times the shear stress). Figure 4(a) shows negative uv (the expected positive shear stress) at large negative z (where the boundary layer is relatively undisturbed by the vortex), but the boundary layer near the centre plane has a large region of negative shear stress in its outer part, as was found in our previous experiments on a weak vortex-pair configuration. Judging from smoke-flow visualization, the vortex sheet from the leading edge has not completely rolled up, so that the vortex over the plate still consists of a core with a surrounding spiral sheet of turbulent fluid, and fluid from the sheet is intermittently found at large enough distances from the core to end up near the centre plane. The part of the sheet that links the two vortices does seem to pass below the plate as intended. Obviously this partly-rolled situation can also be typical of strake-wing aircraft, and we do not propose to change the configuration. To investigate it further, we are starting limited conditional-sampling measurements, in which the selected parts of the flow are slightly heated to act as a "tracer".

There is a change of sign in \overline{uw} (fig. 4(b)) from just above to just below the vortex core. Although not entirely clear in the

coarse-grid measurements shown here, there also seems to be a rapid change of sign of \overline{uv} from just to the left to just to the right hand side of the vortex: this combined behaviour of \overline{uv} and \overline{uw} represents a circumferential transport of u-component momentum, probably corresponding to a natural spiralling motion of the vortex core. The \overline{uw} contours also show up the presence of the "tongue" on the negative-z side of the vortex, together with rather small values everywhere else except immediately above and below the vortex core. The cross-plane shear stress \overline{vw} , shown in figure 4(c) has a rather complicated distribution of maxima and minima with a very strong y-wise gradient through the vortex core, (we suspect that more closely-spaced measurements in the core region, planned for the near future, would show up this strong z-wise gradient also). Figure 5 shows contours of turbulent kinetic energy, the region of comparatively large turbulent energy outside the boundary layer near the centre plane being a further indication of the curious state of the flow in this region.

Finally, as an example of some of the more complicated quantities that we have measured, figure 6 shows the vector whose components are $\overline{q^2_v} / \overline{q^2}$ in the y direction and $\overline{q^2_w} / \overline{q^2}$ in the z direction where $q^2 = u^2 + v^2 + w^2$, and which may be interpreted as a vector plot of the turbulent diffusion velocity in the y-z plane. In an undisturbed boundary layer, the diffusion velocity is of course directly away from the surface but, as can be seen from the "vectors" at $z=-12$, the values are very small compared to those in the vortex flow. The general trend is of course for diffusion away from the vortex region

into the outer, undisturbed flow, but the very strong diffusion into the low-energy region at $-6 < z < -2$, $y=1$, is remarkable, as is the very strong diffusion downwards into the boundary layer near the centre plane.

Plans for September 1985 - March 1986

Fill-in traverse and limited conditional sampling measurements on the current configuration should be complete shortly, and we will proceed to what is probably the less difficult configuration in which the vortex remains clear of the boundary layer for most of the distance down the test plate. We intend to replace the IBM PC clone, which is rather slow, by an existing 8086 machine with a built-in high-speed converter. However, we hope that this will not involve significant amounts of contract staff time. We hope to interest an undergraduate student in flow-visualization work in more practical configurations, including a study of vortex breakdown: however, undergraduate course scheduling means that little work will be done until the next year of the contract.

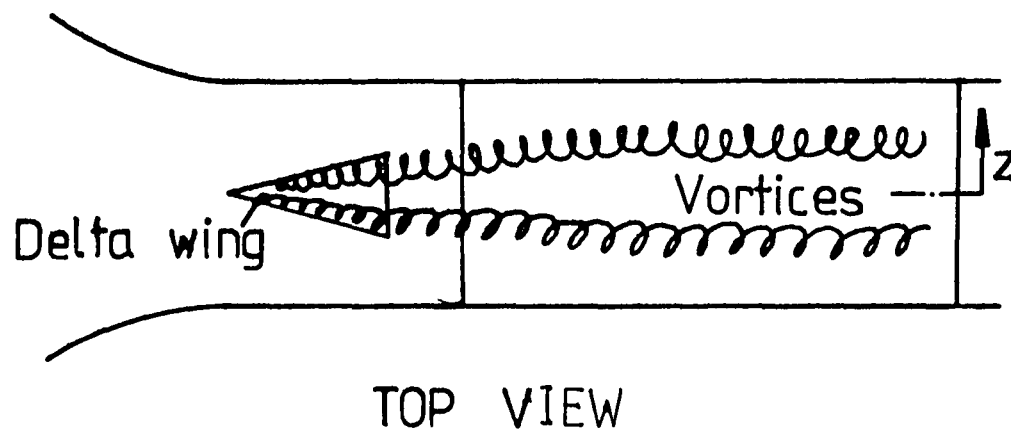
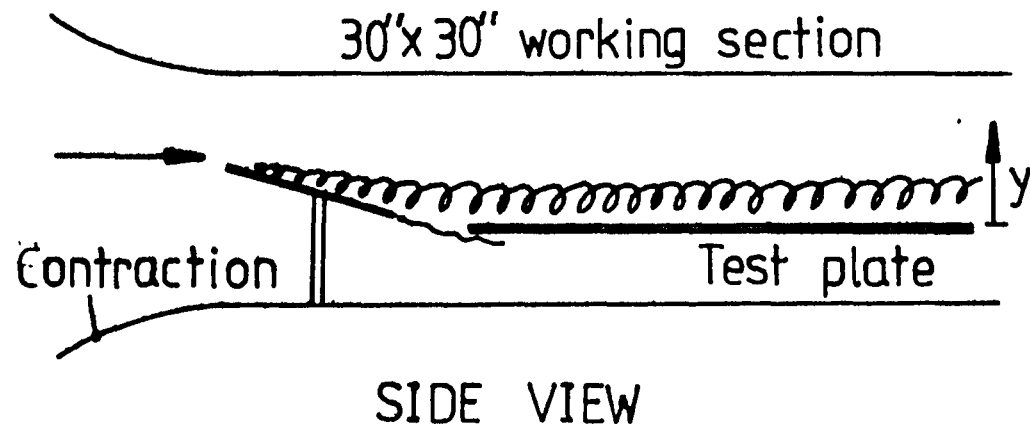


Figure 1. Test configuration with 76 deg. sweep delta wing of 267 mm (10.5 in.) span in 30 in. x 30 in. tunnel. The delta wing is one span ahead of the test plate.

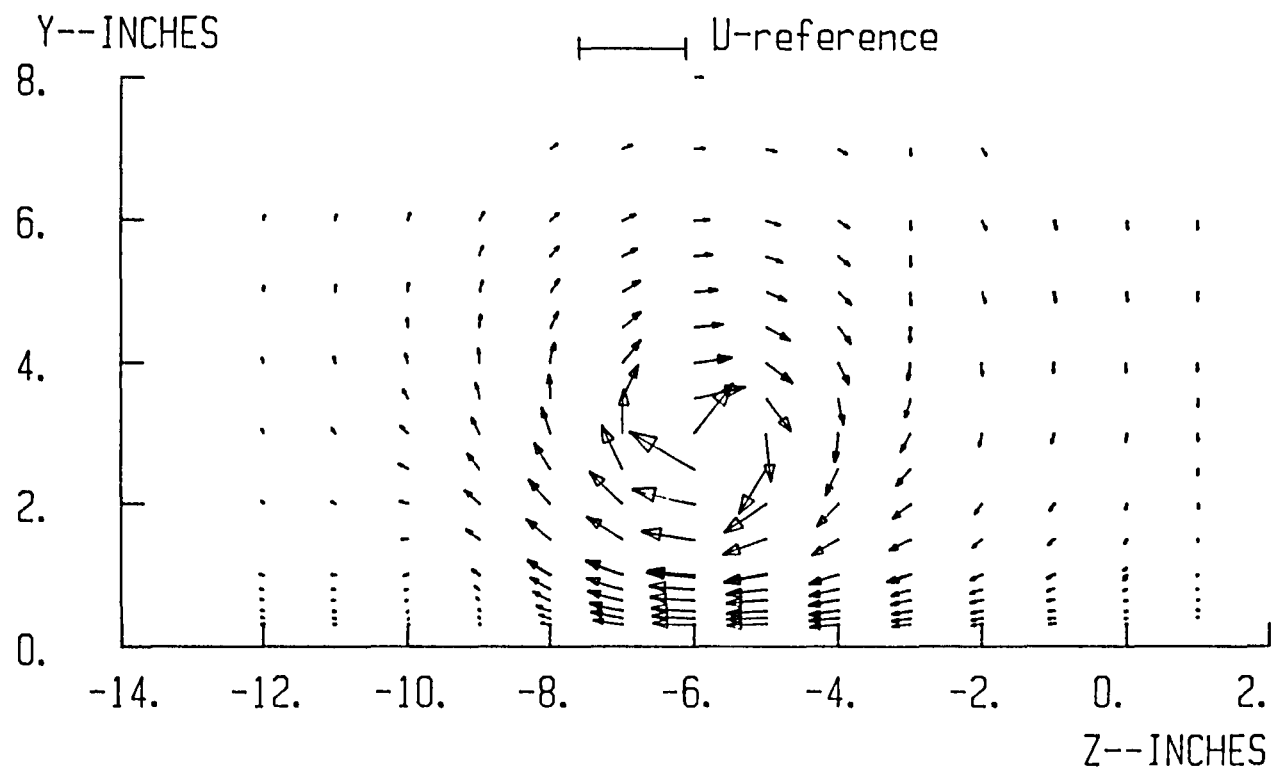


Fig. 2(a) MEAN V-W VELOCITIES
X=34.25 INCHES
U-REFERENCE=20 M/S

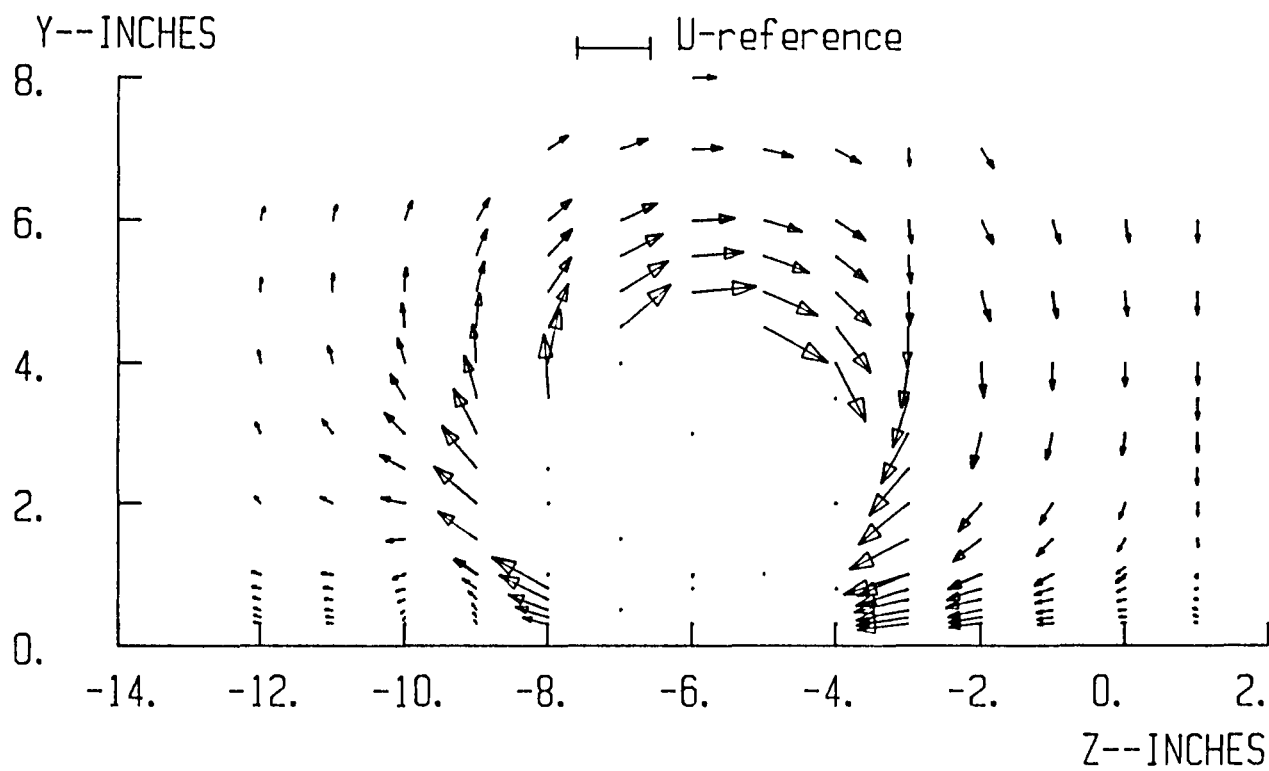


Fig. 2(b) MEAN V-W VELOCITIES

X=34.25 INCHES

U-REFERENCE=5 M/S

Y--INCHES

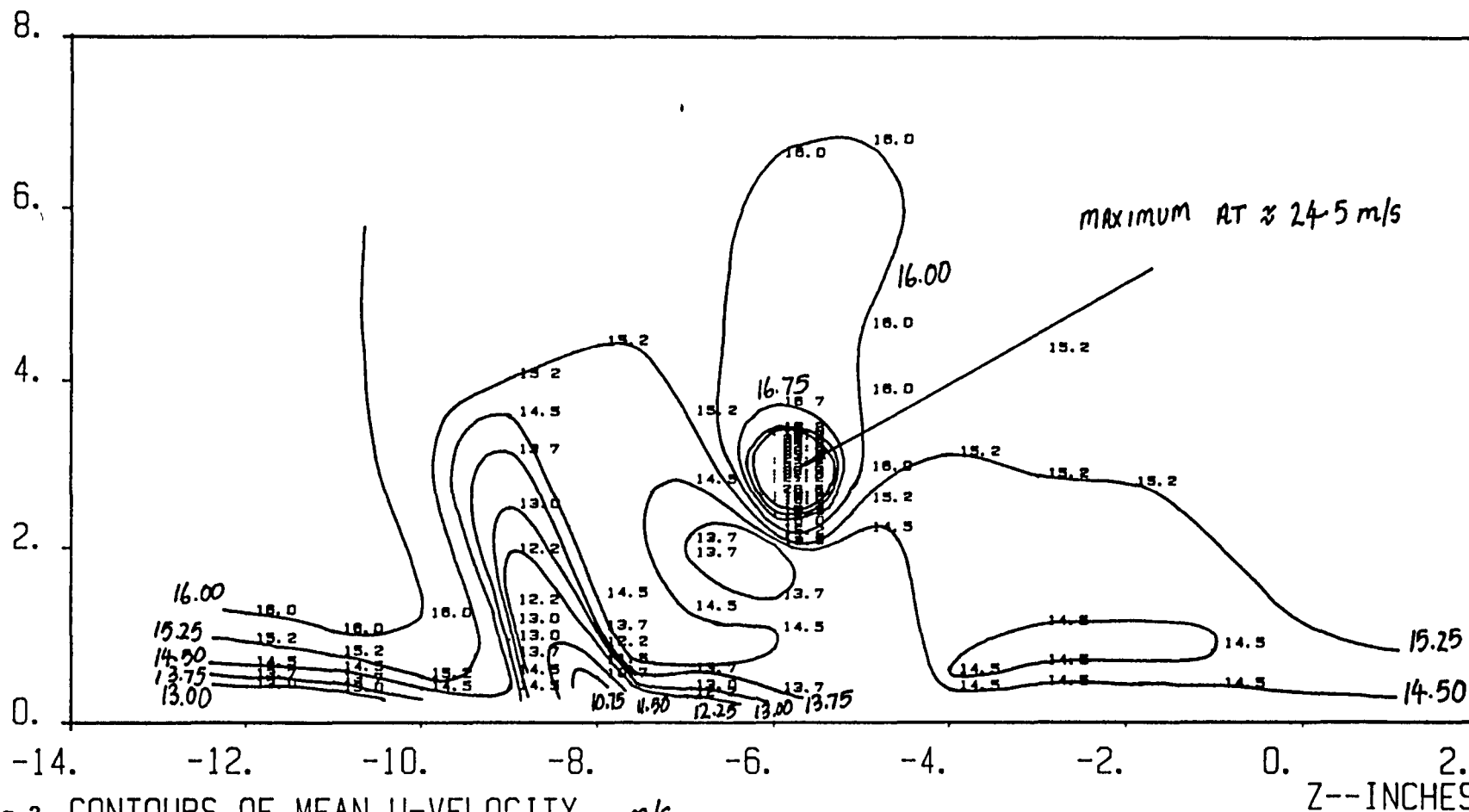


Fig.3 CONTOURS OF MEAN U-VELOCITY - m/s

X=34.25 INCHES

Y--INCHES

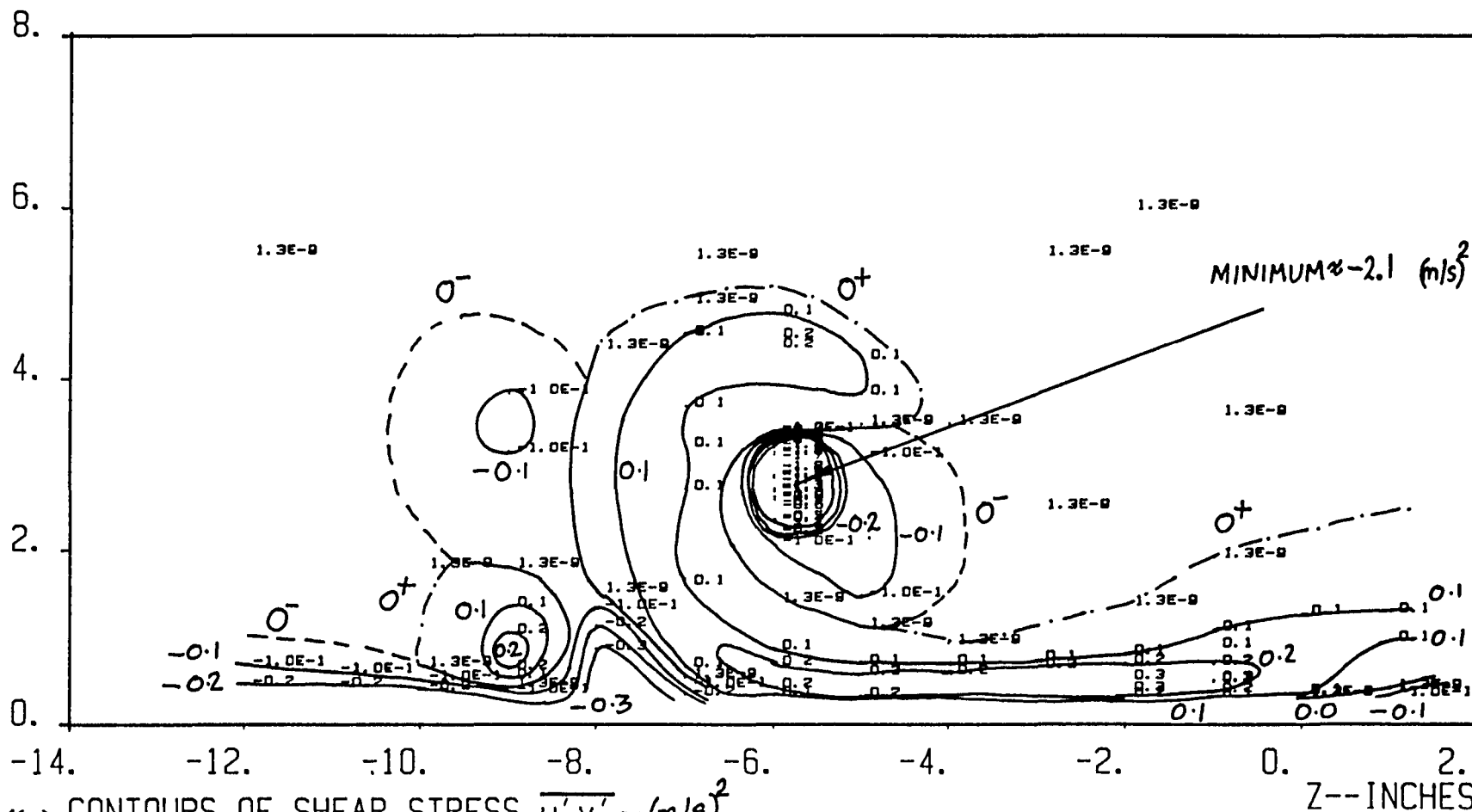


Fig.4(a) CONTOURS OF SHEAR STRESS $\overline{U'V'} - (m/s)^2$
X=34.25 INCHES

Y--INCHES

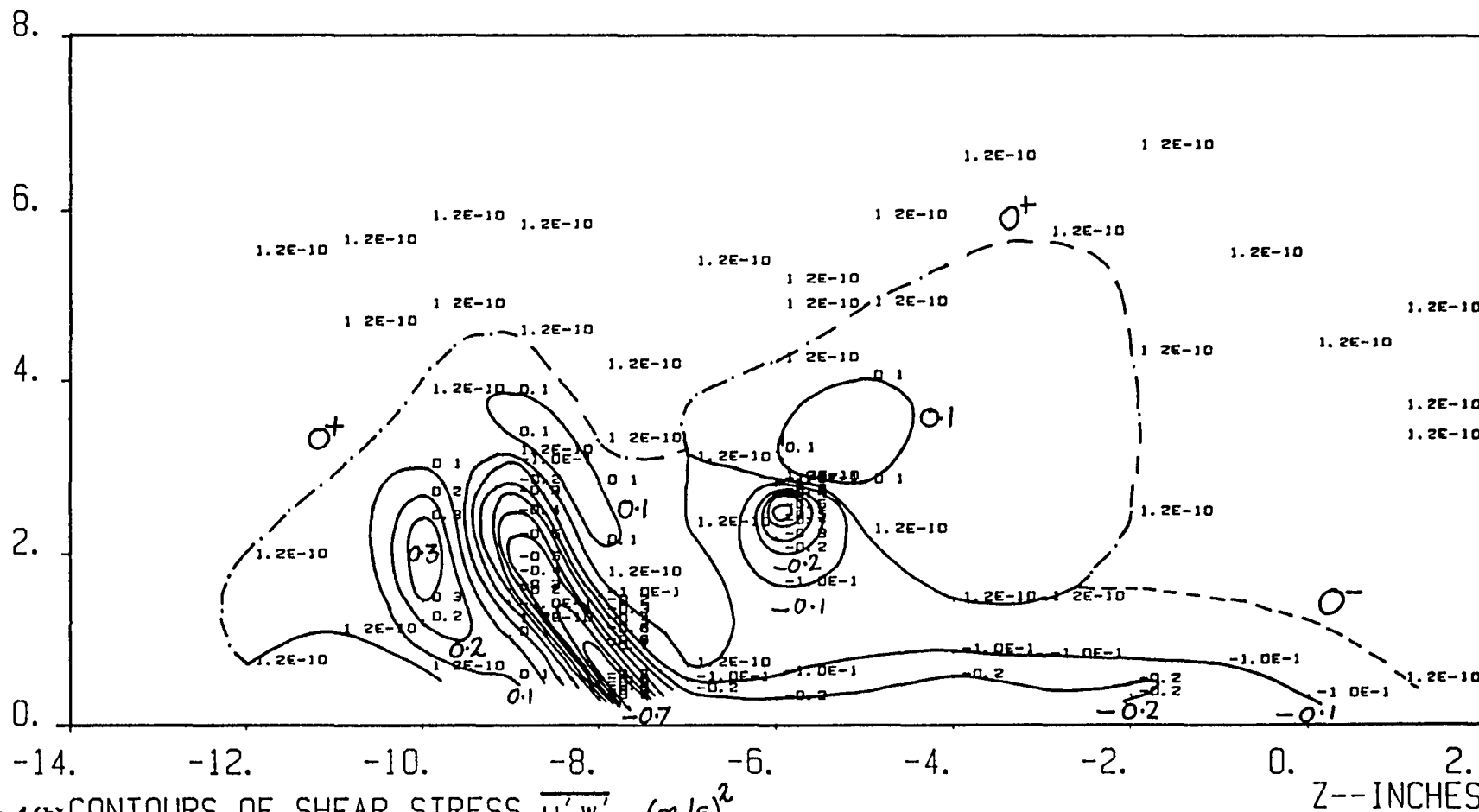


Fig.4(b) CONTOURS OF SHEAR STRESS $\overline{u'w'}$ — $(m/s)^2$

X=34.25 INCHES

Y--INCHES

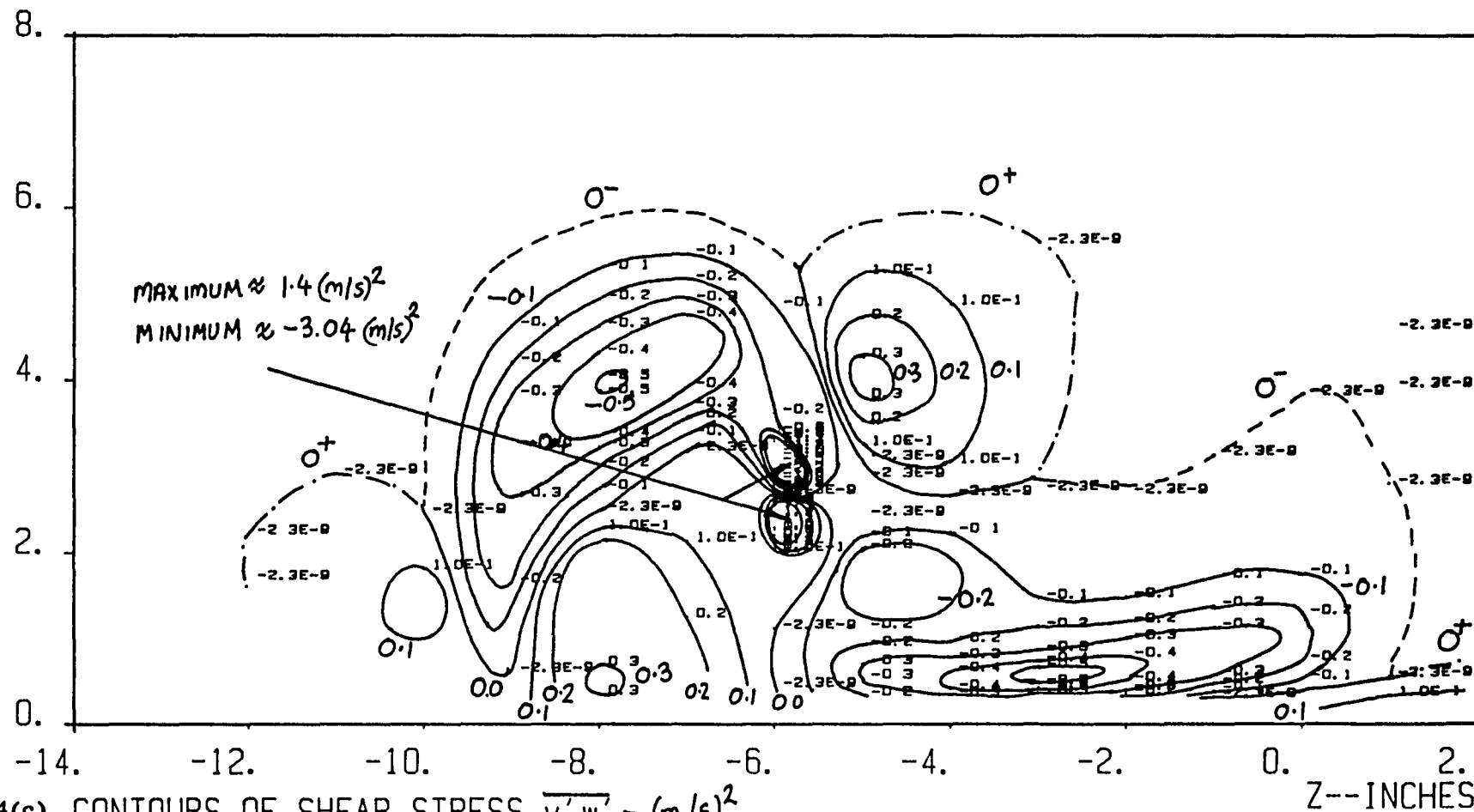


Fig.4(c) CONTOURS OF SHEAR STRESS $\overline{v'w'} - (m/s)^2$

X=34.25 INCHES

Y--INCHES

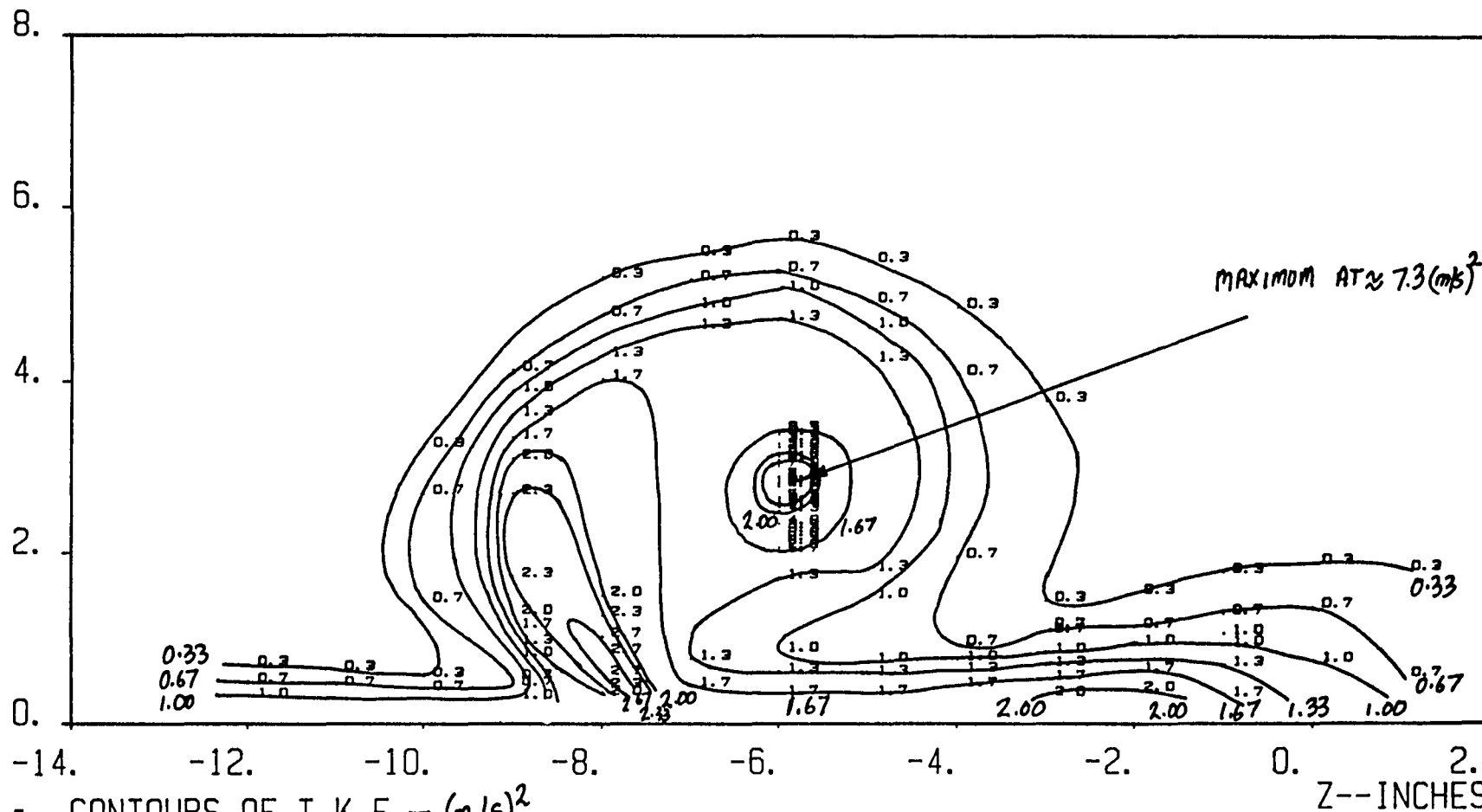


Fig.5 CONTOURS OF T. K. E. - $(m/s)^2$
X=34.25 INCHES

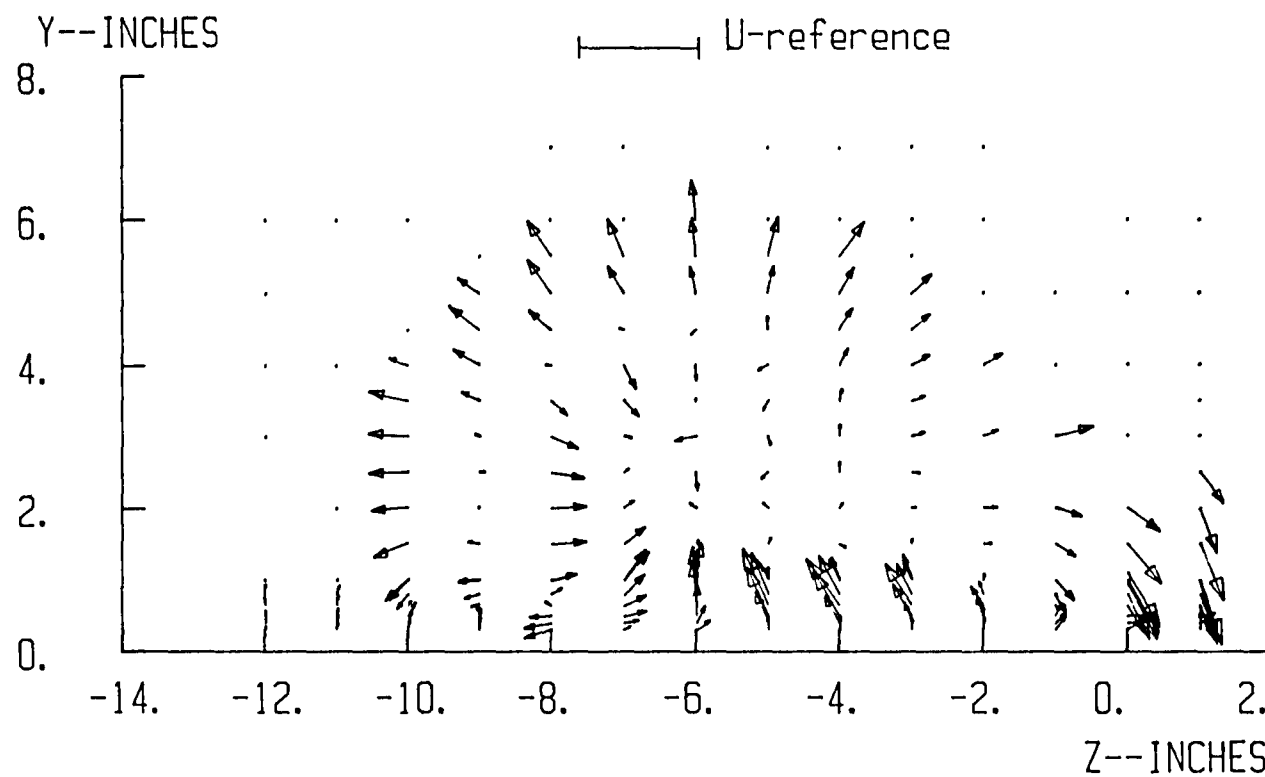


Fig.6 T.K.E. DIFFUSION VELOCITIES
X=34.25 INCHES
U-REFERENCE=2 M/S

End of Document